buildings

MDPI

Article

Framework for a City's Performance Assessment in the Case of an Earthquake

David Koren and Katarina Rus *

Faculty of Architecture, University of Ljubljana, 1000 Ljubljana, Slovenia
* Correspondence: katarina.rus@fa.uni-lj.si

Abstract: A comprehensive assessment of a city's vulnerability and resilience is a prerequisite for an effective response to a natural disaster, such as an earthquake. However, an appropriate method for assessing the seismic performance of a complex urban system is still being researched. To address this gap, the purpose of this paper is to introduce a method for seismic performance assessment of a city as a socio-physical system. Therefore, various studies of individual urban components and their interactions were combined into a holistic framework and presented in a case study of a small mid-European town. The seismic vulnerability of the building inventory was assumed or assessed based on the fragility curves adopted from the literature on similar European building stock. Seismic scenarios of different earthquake intensity (PGA of 0.15 g and 0.30 g) combined with conservative and risky approaches were applied. Considering the human perspective, urban performance was evaluated on the basis of accessibility to urban services that satisfy basic human needs (for survival and protection) via graph theory measures of global efficiency and the shortest path. The temporal aspect (before the earthquake, immediately after it, after evacuation, and after recovery) was also included to obtain a comprehensive resilience assessment. It turned out that a stronger earthquake (PGA of 0.30 g) would have far-reaching consequences for the urban performance of the investigated town, and the old city center would be particularly affected. Following the event, the system's performance is less than half as effective compared to the initial level, indicating a sharp deterioration in the quality of life as reflected in the possibility of meeting basic human needs.

Keywords: earthquake; urban system; urban performance; accessibility; human needs; resilience

Citation: Koren, D.; Rus, K. Framework for a City's Performance Assessment in the Case of an Earthquake. *Buildings* **2023**, *13*, 1795. https://doi.org/10.3390/buildings13071795

Academic Editor: Xavier Romão

Received: 29 May 2023
Revised: 10 July 2023
Accepted: 11 July 2023
Published: 14 July 2023

1. Introduction

Civilizations throughout history have been threatened by various natural disasters. However, due to world population growth and rapid urbanization in recent decades, we have witnessed increasingly severe consequences of these extreme events. Among them, earthquakes proved to be the most extensive in terms of casualties, economic loss, and a decrease in the overall quality of urban life. Moreover, even though an earthquake is a rare event with a low probability of occurrence, its unpredictable nature makes the planning of seismically resilient urban systems very challenging.

In order to understand the seismic behavior of structures and thus prevent or at least mitigate fatal consequences, many studies and seismic analyses of the built environment have been carried out [1–8]. In recent decades, extensive research and significant advances have been made in modeling, analysis, design, and behavior assessment at the individual structure level as well as on the macro-urban [3,6,8], regional [5,9], and even world scales [2].

The analysis of a complex urban system is accompanied by many uncertainties and limited data on physical structures, social environments, and local ground motions. It is practically impossible to obtain the exact data on all the details of the entire urban system at a macro level. Therefore, an approach to classifying buildings into different classes based on rough data has been established [10]. The most important basic building attributes [11] are construction material, the lateral-load-resisting system, the period of construction, and building height (i.e., the number of floors) [12]. Furthermore, it is possible to create more detailed classes if we have the data on horizontal structure (e.g., vaults, flexible/rigid slabs), vertical structure (regular/irregular layout), and rods or beams (tie or not) [13,14]. Each class groups together buildings with the same properties that are characterized by similar seismic behavior and a comparable extent of damage caused by an earthquake. The occurrence probability of a certain damage level for an individual building class is described by the fragility curve. Various studies have examined the derivation of fragility curves for specific types of structure, which can be assigned to each building class. Generally, two main methods, namely empirical and mechanical, are employed for the derivation of fragility curves [15,16]. Among empirical methods [14,17–20], fragility functions are derived by establishing a relationship between observed damages and specific seismic events. This involves statistical data processing to assess the probability of a particular damage state occurring depending on the intensity measure (IM). On the other hand, specific analyses using numerical models are employed in mechanical methods [21–24] for the derivation of fragility functions. Besides these main methods, a hybrid approach [13] combines empirical data and mechanical models to derive fragility functions. The use of corresponding fragility curves for a specific building class enables us to move from the seismic vulnerability analysis of individual buildings to the assessment of the building stock as a whole [8,25–29].

Often, studies dealing with the seismic vulnerability of built structures on the urban level refer to two European projects from the beginning of the 21st century. The essential contribution of the RISK-UE project [6,17] is the typology classification of selected European-type buildings. Another European project, Syner-G [3,30], offers systemic seismic vulnerability and risk analysis of buildings, lifelines, and infrastructures. Moreover, the project aimed to create a Fragility Function Manager tool for large-scale vulnerability assessment including the fragility curve library [30]. However, it is worth mentioning that due to all the various factors influencing the seismic response of structures in relation to both structural and foundation components (e.g., steel and confinement ratios, shear walls, soft-stories, irregularities, foundation dimensions, and types), the accuracy of fragility curves may differ considerably [31]. To address the issue of inaccuracy, recent studies have tried to move beyond the rough building classification by suggesting various supplementations and additional criteria for a more precise vulnerability evaluation [25,32,33].

In addition to the seismic response of built structures, their influence on other urban components is another crucial aspect for evaluating a city's performance. The interconnectivity and interdependencies of different urban components (buildings, infrastructure, open spaces, the social component [34]) create efficient service delivery, but the failure of one component may result in cascade effects with severe consequences. Therefore, some studies deal with the impact of buildings on the road transportation infrastructure [35,36] and interdependency between critical infrastructure [37], while others address social influences [38,39] and the significance of open spaces [40–42]. However, a holistic approach to the assessment of a city's seismic performance should encompass the complexity of an urban system as a whole, including its main physical and social components and the dynamic interactions between them [34].

A city's performance is a general notion observed from several aspects, ranging from engineering and economic features to social factors. From a human perspective, an efficient urban system is perceived as a place of prosperity that supports the well-being of its inhabitants. The quality of life and overall life satisfaction of residents depend on their ability to meet basic human needs [43,44]. Therefore, a city's performance from a human perspective could be measured by the accessibility of urban services that satisfy these needs [45–48]. Shang et al. [49] introduced a framework for post-earthquake accessibility of healthcare services considering the seismic damage to buildings and transportation networks, as well as post-earthquake availability of patient beds and medical staff. On the other hand, Cavallaro et al. [50] present a city as a 'Hybrid Socio-Physical Network' (HSPN) and evaluate its performance via mutual accessibility by applying the graph theory measure of global efficiency. They do not take individual needs into account, which is discussed by Pan et al. [46]. The latter paper presents an approach based on the 'Restored Quality of Life'(REQUALIFE) and the 'post disaster quality of life—PQL' measure for urban performance. PQL is a composite indicator based on the Maslow theory of basic human needs, which proposed the hierarchy of needs. However, in recent social and psychological studies, the traditional hierarchy has been replaced by a more flexible system of needs that depends on an individual's preferences [51]. In addition, the PQL indicators, as well as the desired performance, are dependent upon subjective decisions made by the expert group conducting a specific case study. Therefore, the PQL is not a universal method and does not allow for comparisons between different cities.

Various external and internal factors, including earthquakes and other natural disasters, influence the performance of an urban system over time. However, resilient cities can maintain access to services and facilitate the fulfillment of basic needs during and after hazard events.

The purpose of this study is to comprehensively evaluate a city's seismic performance from a human perspective by applying objective measures while also considering the time aspect (before the event, immediately after it, and during the recovery phase). Therefore, the main aim of the paper, i.e., a framework for assessing a city's performance by measuring the accessibility to basic human needs, is introduced in the following sections.

2. Proposed Framework for the Seismic Performance Assessment of an Urban System

The presented proposal for the urban seismic performance assessment combines various existing studies and their findings, which partially address the topic, and compiles them into a comprehensive framework. The framework aims to assess the overall system functionality on the basis of individual components and their interactions. Combining component fragility with system fragility involves integrating the failure probabilities or fragilities of individual components within a larger system-level analysis. By analogy with engineering methods that estimate the probability of damage to structural systems consisting of interrelated components [15,52], the process for evaluating seismic vulnerability at the macro urban level was applied. The process typically consists of the following steps: identification of components, determination of component fragility, accounting for interdependencies, and combining component fragilities into system fragility. The proposed framework is presented step-by-step in the following subsections and illustrated in Figure 1.

2.1. Identification of Urban Components under Investigation

The suggested framework was tested on a model of the small mid-European town of Brežice. It is located in the earthquake-prone southeast part of Slovenia, where the expected design ground acceleration according to Eurocode 8 (soil type A, return period 475 years) is up to 0.30 g [53]. According to 2020 census data [54], the town of Brežice has almost 7000 inhabitants and features a health center and two fire stations. The town's origins date back to the Middle Ages, and the old town center and a castle from the 13th century are still preserved.

All data for the performed analysis of the built environment's seismic vulnerability and the assessment of urban system performance were publicly available. Most of the data were obtained from the Geodetic Administration of the Republic of Slovenia (GURS) [55] and the Open Street Map [56]. Basic building attributes for seismic vulnerability assessment of building inventories considered in this study were construction material, height (the number of stories), age (the period of construction), location, footprint (the gross floor area), and use (residential, non-residential, healthcare, and emergency buildings). However, no data on the lateral-load-resisting systems of the buildings, which are the crucial characteristics in the structural seismic analyses, can be found within these databases. For road transportation infrastructure, the data on the location, footprints, total length and width, and length of individual links were applied.

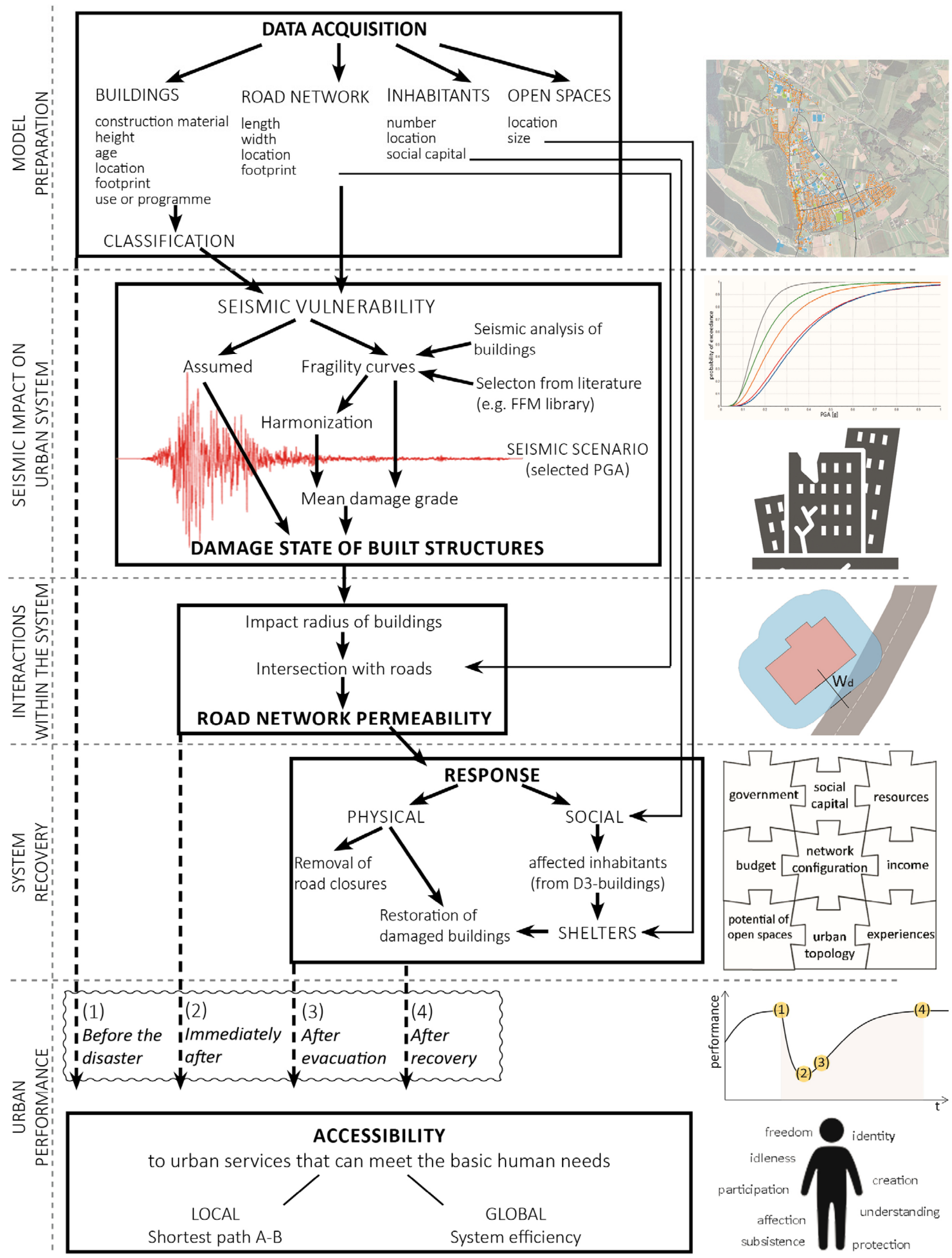

Figure 1. A flowchart of the presented framework for urban seismic performance assessment.

The number of inhabitants of each building was calculated on the basis of census data. In the study, the inhabitants were assumed to be uniformly distributed according to the total floor area of the buildings (buildings' footprints area multiplied by the number of stories) while considering that population density in multi-residential buildings is two times larger than that of single houses.

Finally, the test model with 6843 inhabitants contained 1446 buildings, 1069 of which were residential. Most of them were masonry and low-rise buildings constructed in the second half of the 20th century (Figures 2 and 3). Among non-residential buildings, 18 were recognized as important buildings for the provision of healthcare and emergency services. The urban system was connected by a network of roads (from minimum 2 m to maximum 18 m in width) with a total length of 50.76 km, which enable accessibility to various urban services.

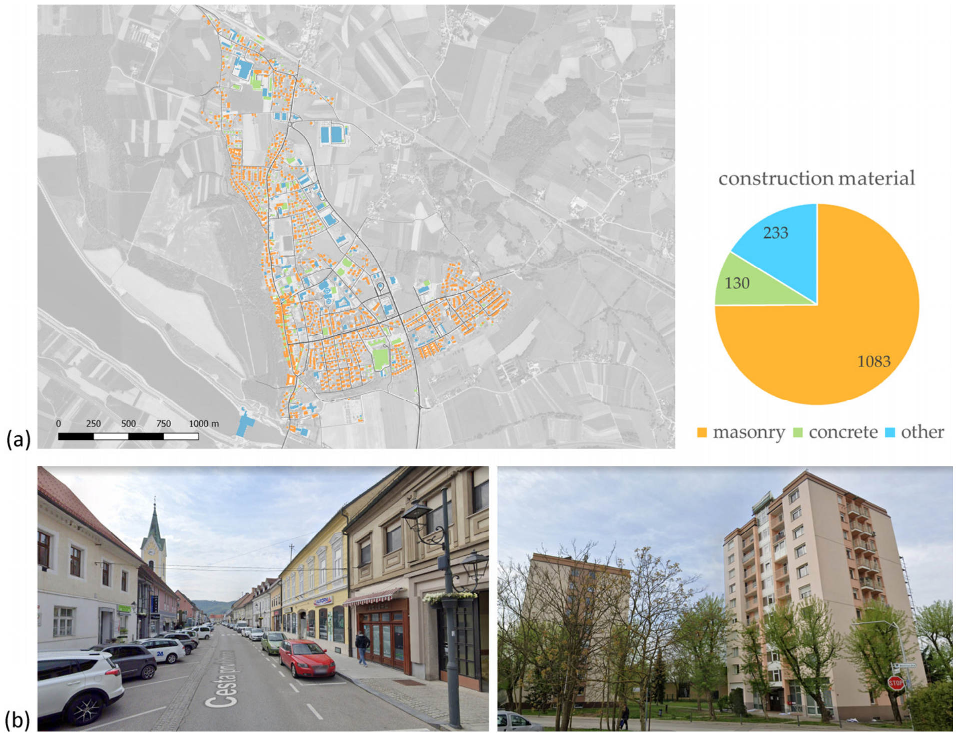

Figure 2. The case study of the town of Brežice: (**a**) distribution of buildings according to construction material; (**b**) typical street and buildings (left masonry, right RC) [57].

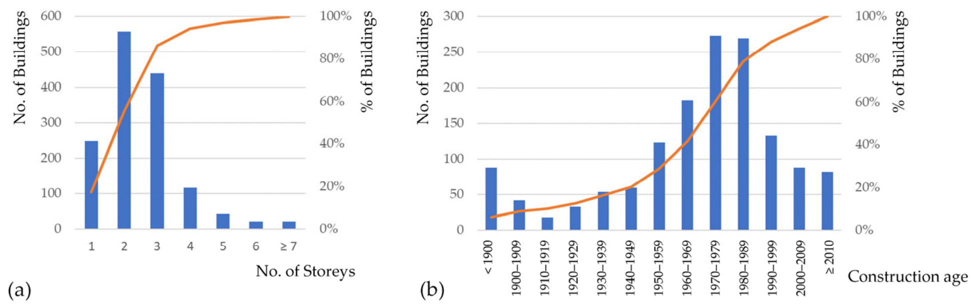

Figure 3. Distribution and cumulative percentage of 1446 buildings when accounting for the number of stories (**a**) and the period of construction (**b**).

2.2. Classification of Buildings

An accurate seismic performance analysis of even a single structure is a complex, data-demanding, and time-consuming procedure. Therefore, for a large-scale analysis of building stock, many simplifications are usually introduced, e.g., the grouping of buildings with similar properties. Accuracy depends on data availability, the scope of analysis, and the details of a particular case study.

In the event of an earthquake, buildings within the same class can be expected to exhibit similar responses as the level of damage is dependent on the material of construction, the lateral-load-resisting system, and construction quality. The failure mechanisms could be either local or global and primarily depend on the type of construction, materials used, structural configuration, and the intensity and characteristics of the seismic event. For example, some of the most common failure mechanisms of RC structures are flexural, shear, or bond failures and rocking, sliding, or collision mechanisms, while for common masonry structures, the most characteristic failure mechanisms are shear and diagonal tension failures and out-of-plane failures of the walls [58–64]. According to failure mechanisms, various taxonomies of building classes that share a common division according to the basic criteria for buildings classification have been introduced: the construction material, lateral-load-resisting system, construction period, and number of floors [12]. Most of the existing taxonomies are focused on local design and construction practices. Among them, ATC-13 [65] and HAZUS [66] were developed for the construction types present in the United States, while in Europe, the RISK-UE [6] and Syner-G [30,67] taxonomies have been developed and applied. A few taxonomies have a global focus and applicability, for instance, the recently developed GED4ALL taxonomy that offers a comprehensive, modular, and flexible classification system to characterize single buildings or building classes for multi-hazard risk assessments [12]. In addition to the classification of buildings, it offers an open exposure database schema for road networks, other infrastructural systems (railway networks, bridges, pipelines and storage tanks, power grids, energy generation facilities), crops, livestock and forestry, and socio-economic data [68].

In our case, the Syner-G taxonomy was adapted due to its compatibility with the Fragility Function Manager program, which was employed for vulnerability assessment (see Section 2.3.1). The investigated building inventory was divided into 12 classes according to the construction material, construction period, and the number of floors. Moreover, an extra class for important buildings (which are used for the provision of healthcare and emergency services) was set up (Table 1). The construction materials taken into consideration included masonry (M), reinforced concrete (RC), and other materials (O). In terms of height, low-rise (1–3 stories), mid-rise (4–6 stories), and high-rise (7 stories or more) buildings were recognized. Another significant feature for the classification of buildings is the age of construction, which indicates different building codes, quality of materials, and practices in each period. In the region of Slovenia, there were major changes in the seismic building standards in the periods of 'before 1964', '1965–1981', and 'after 1982' [69]. In the case of masonry buildings, we did not consider the age of the structure because the set of fragility curves in the FFM library (which were used for the purpose of this study; see Section 2.3.1) does not distinguish between the quality of seismic construction and only addresses the type of structure with regards to the high and low percentage of voids. Therefore, we used this information to apply a risky (low percentage of voids) and a conservative (high percentage of voids) approach in order to determine the spectrum of possible outcomes. In this case study, there were no high-rise masonry buildings or RC buildings built before 1964. Regarding other buildings, the only relevant data were related to the date of construction (before 1981 and after 1982). It is worth noting that for the investigated building inventory there were no publicly available data regarding the types of the buildings' lateral-load-resisting systems and limited data on materials other than masonry and concrete.

Finally, healthcare and emergency facilities, which can ensure the fulfilment of the citizens' needs for survival and protection, were recognized as the most important non-residential buildings in the case of an earthquake. In the study, they were divided into a separate class of important buildings (IBs). After an in-depth review of IB data, it was found that all of these buildings were renovated after 1982 when strict seismic building codes were put in place. Therefore, important buildings were assumed to be seismically safe (i.e., achieved the D1 damage state and remained unaffected and functional) in the event of an earthquake with a design ground acceleration (0.30 g).

Table 1. The characteristics of analyzed building stock: classification of buildings, their seismic vulnerability, and most probable seismic response in assumed seismic scenarios presented in terms of the damage distribution [%] and mean damage grade μ_D.

Class	Material	Height	Age	0.15 g										0.30 g										Sum	%
				Risky					Conservative					Risky					Conservative						
				D1	D2	D3	μ_D		D1	D2	D3	μ_D		D1	D2	D3	μ_D		D1	D2	D3	μ_D			
ML	masonry	low-rise		64.7	28.7	6.6	1.42	**D1**	52.8	32.3	14.3	1.62	**D2**	19.9	39.2	40.9	2.21	**D2**	12.8	30.1	57.2	2.44	**D2**	921	63.7
MM		mid-rise		43.9	47.5	8.6	1.65	**D2**	31.9	40.8	27.3	1.95	**D2**	9.2	31.1	59.7	2.51	**D3**	4.8	15.0	80.3	2.76	**D3**	151	10.4
RCL00	reinforced concrete	low-rise	before 1964	40.1	51.5	8.4	1.68	**D2**	40.1	51.5	8.4	1.68	**D2**	10.2	52.7	37.1	2.27	**D2**	10.2	52.7	37.1	2.27	**D2**	11	0.8
RCL65			1965–1981	56.0	38.8	5.2	1.49	**D1**	56.0	38.8	5.2	1.49	**D1**	17.6	53.9	28.5	2.11	**D2**	17.6	53.9	28.5	2.11	**D2**	33	2.3
RCL82			after 1982	73.4	24.9	1.6	1.28	**D1**	73.4	24.9	1.6	1.28	**D1**	33.9	51.5	14.6	1.81	**D2**	33.9	51.5	14.6	1.81	**D2**	49	3.4
RCM00		mid-rise	before 1964	52.3	42.6	5.1	1.53	**D2**	52.3	42.6	5.1	1.53	**D2**	6.8	52.4	40.9	2.34	**D2**	6.8	52.4	40.9	2.34	**D2**	1	0.1
RCM65			1965–1981	80.9	17.1	2.1	1.21	**D1**	80.9	17.1	2.1	1.21	**D1**	32.2	43.5	24.3	1.92	**D2**	32.2	43.5	24.3	1.92	**D2**	5	0.4
RCM82			after 1982	93.1	6.2	0.7	1.08	**D1**	93.1	6.2	0.7	1.08	**D1**	49.1	35.6	15.3	1.66	**D2**	49.1	35.6	15.3	1.66	**D2**	16	1.1
RCH65		high-rise	1965–1981	71.0	25.5	3.6	1.33	**D1**	71.0	25.5	3.6	1.33	**D1**	57.9	35.0	7.1	1.49	**D1**	57.9	35.0	7.1	1.49	**D1**	8	0.6
RCH82			after 1982	79.0	14.3	6.7	1.28	**D1**	79.0	14.3	6.7	1.28	**D1**	66.9	20.3	12.8	1.46	**D1**	66.9	20.3	12.8	1.46	**D1**	2	0.1
O00	others		before 1981	-	-	-	-	**D1**	-	-	-	-	**D2**	-	-	-	-	**D3**	-	-	-	-	**D3**	136	9.4
O82			after 1982	-	-	-	-	**D1**	-	-	-	-	**D1**	-	-	-	-	**D2**	-	-	-	-	**D3**	95	6.6
IB	important buildings renovated after 1982			-	-	-	-	**D1**	-	-	-	-	**D1**	-	-	-	-	**D1**	-	-	-	-	**D1**	18	1.2

2.3. Analysis of Seismic Impact on an Urban System

2.3.1. Application of Fragility Curves

The seismic behavior of structures and the resulting damage can be estimated on the basis of fragility curves. They provide the probability of exceeding different limit states (physical damage or injury levels) given the level of ground shaking (e.g., peak ground acceleration—PGA) for a specific building or a building class [67]. Plenty of studies deal with the derivation of fragility curves [14,15,17,21,22]; thus, a wide range of different curves is available in the scientific literature. When it comes to urban-scale analysis of seismic response, the challenge is to determine the most appropriate curve for each class. In addition to the construction material, height, and the age of a building, the local context is also important when making decisions. Therefore, the Fragility Function Manager (FFM) program was developed as part of the Syner-G project to assist in decision making [30,67]. It contains a library of more than 400 different fragility curves and a filtering tool for selecting the most suitable ones.

In this study, fragility curves for masonry and reinforced concrete classes were selected using the FFM program. Different curves were selected for masonry low-rise and mid-rise structures according to Ahmad et al. [22], also taking into consideration risky (low percentage of voids) and conservative (high percentage of voids) approaches to address uncertainties about structure. For each class of RC structures, a curve was selected based on the ratio (Q/W) of the maximum base shear to total weight [21]. Selected curves introduced by Borzi et al. [21] consider that higher RC buildings are less vulnerable (lower oscillation frequency, minor forces) in terms of the main structural elements. However, in this case (due to a lower stiffness of the primary structure), higher levels of damage to non-structural elements (including façades, etc.) are more likely to occur. Although this mechanism applies to frame structures, which are not so common in the investigated region, these fragility curves were selected as the most appropriate for the presented analysis. For structures made of other materials and for important buildings, no corresponding fragility curves were available in the FFM library. Therefore, their damage states were assumed by making qualitative comparisons according to the recommendations [70].

When selecting fragility curves from different databases and authors, the problem of non-uniform curves often arises. Fragility curves can differ in the number of limit states, measurement units (e.g., ground acceleration), and scale. To unify different types of fragility curves, the process of harmonization provided by the FFM was carried out in this study (Figure 4). It resulted in the set of two curves (yielding and collapse) and three damage states: D1—without damage; D2—slight to moderate damage, still-usable construction; D3—severe damage, non-usable construction. It should be noticed that harmonization does not take into account the out-of-plane failure mechanisms for masonry buildings. However, it only has a minor impact on the overall seismic assessment of an urban system because, in most cases, yielding and out-of-plane curves have a rather similar shape. The most noticeable difference (15%) between the two values of probability exceedance for the yielding and out-of-plane mechanism was in the case of low-rise masonry buildings in the 0.30 g scenario. In all other cases, the values did not differ by more than 7%, while in the case of mid-rise masonry buildings and the 0.30 g conservative scenario, both values coincided. The influence of buildings that reached the D2 damage state on other urban components was captured in the calculation of the impact radius, which also includes the impact of out-of-plane failure. However, for a more precise analysis, an out-of-plane mechanism should be taken into consideration as well.

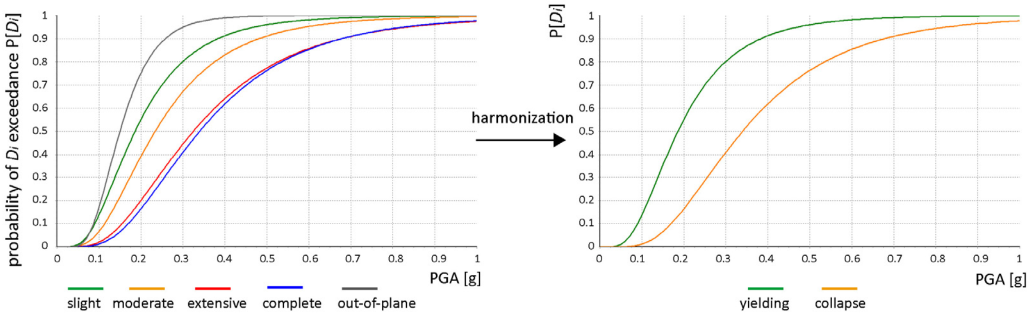

Figure 4. Fragility curves' harmonization process based on the example of a low-rise masonry building class with a low percentage of voids [22].

2.3.2. Considered Earthquake Characteristics

An earthquake is a complex natural event that is challenging to simulate. Seismic scenarios encompass various earthquake rupture characteristics, such as magnitude, hypocenter location, fault type, and soil type. It should generate a distribution of intensity measures (such as PGA) that is not uniform at a given location. However, due to the scope and constraints of our research, we simplified the definition of seismic scenarios. Two different scenarios with uniformly distributed PGA across the entire investigated area were assumed based on the design ground acceleration for the particular location. Moreover, due to the relatively small area of analysis (ca 3.5 km^2) and the uniform type of soil [71], the results of the study were not affected by soil amplifications. A severe earthquake with a PGA of 0.30 g (the design PGA for the case study location [53]) and a moderate seismic event with a PGA of 0.15 g (half the design PGA) were considered. Each scenario was analyzed according to a risky and a conservative approach to determine the possible range of consequences. In the case of masonry buildings, we obtained two fragility curves for each class for a low percentage of voids (the risky approach) and a high percentage of voids (the conservative approach). With regards to RC buildings, the same fragility curves were used both for the risky and the conservative approaches because the percentage of voids in relation to the RC structures is irrelevant. When dealing with other building classes, a difference of one damage state was assumed between the risky and the conservative approaches. However, important buildings (IBs) were considered as being totally earthquake-resistant in selected scenarios as all these buildings had undergone renovations in the recent period (after 1984), during which modern building regulations specifically addressing earthquake-resistant construction were already in force. Both scenarios were considered as night-time events, and all inhabitants were expected to be at home (in residential buildings), while non-residential buildings were presumed to be empty at the time when an earthquake struck.

2.3.3. Assessment of Building Damage and Its Distribution within the System

The average damage state of buildings belonging to a certain class can be determined on the basis of fragility curves. For the selected PGA, it is possible to extract the damage distribution of the observed building class (Figure 5). Every curve depicts the limit between different damage states and the probability of exceeding the state below the curve. The area between two limit state curves represents a certain damage state and its probability as a function of the level of ground shaking (PGA). At a selected PGA, it is possible to read the proportion of the damage state for a certain building class.

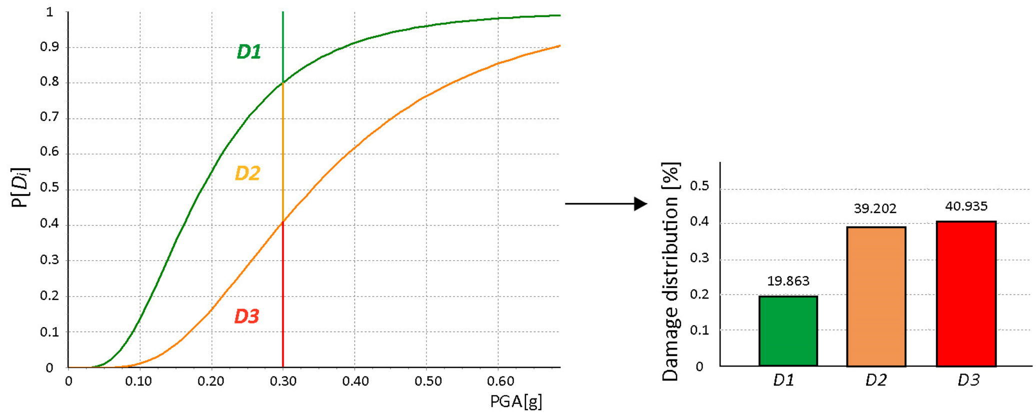

Figure 5. Damage distribution for the low-rise masonry building class considering the risky approach (low percentage of voids) [22] derived from harmonized fragility curves.

On the basis of the damage distribution, it is possible to determine the most likely state of damage for each building class at the selected level of ground shaking (Table 1). It was calculated by applying Equation (1) for the mean damage grade [17]:

$$\mu_D = \sum_{k=0}^{n} p_k k \quad (1)$$

where p_k means the probability of achieving the damage grade D_k and index k runs from 1 to n (the number of all damage states), which is 3 in our case study.

On the other hand, no fragility curves were assigned to building classes of other construction materials (O00 and O82) and important buildings (IB). Therefore, considering no damage distribution, one constant damage state for these classes was assumed in this study.

2.3.4. Interaction between Buildings and the Road Network

An earthquake has a direct impact only on built structures, while other urban components are affected indirectly. To assess the damage to other components, interactions with buildings and the influence of the building stock on them should be considered. In this regard, this study was limited to the influence of buildings on transportation infrastructure and its consequences for accessibility to urban services that can satisfy the inhabitants' basic needs for survival and protection. Firstly, the influence of built environment on the road system was evaluated by calculating the impact radius of each building [35]:

$$W_d = \sqrt{W^2 + \frac{2k_v WY}{\tan\ c}} - W \quad (2)$$

where W_d is the debris width (i.e., potential damage to the building in the case of a severe earthquake) and W is the width of the building (Figure 6). Additionally, k_v, Y, and c are assumed factors taken from Koren and Rus [72], where k_v is the ratio between the collapsed volume and the original volume of the building, Y is the building height, and c is the inclination of the collapse.

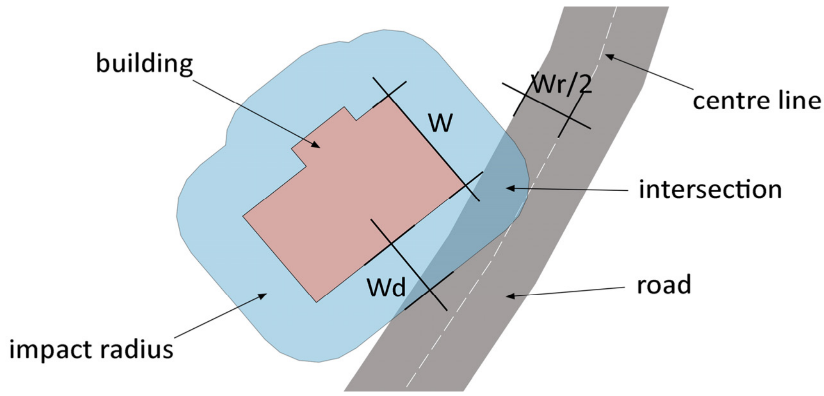

Figure 6. Impact radius of a damaged building and its influence on the road network.

When the impact radius was calculated, its intersection with the road network was analyzed (Figure 6). Each road segment was given a level of permeability (Pi). It was defined as the proportion of road blockages, where W_r is the road width. Where the impact radius of the damaged building W_d extends beyond the middle of the road segment ($W_r/2$), the segment was defined as blocked and impassable (P3). Where the impact radius does not reach the middle of the road segment, the road was treated as partially blocked (P2). Finally, the average travel speed (by car) on the road segment was defined for completely permeable road segments [73], and for partly permeable segments, the half-value was used (Table 2).

Table 2. Determining the influnece of a damaged building on a nearby road segment—assumed levels of road blockage, road permeability, and average travel speed by car.

Intersection	Road Blockage	Road Permeability	Average Speed [km/h]
0	no	P1	20
$<W_r/2$	partial	P2	10
$>W_r/2$	total	P3	0

2.4. Analysis of Urban Performance

Urban systems are the result of human aspirations for efficient, pleasant, and comfortable living. Their main purpose is to create an environment for satisfying various human needs. Cities offer an opportunity to fulfill these needs, but it is up to its inhabitants and other users to take advantage of it. Therefore, a city's performance is observed from a human perspective according to the satisfaction of basic human needs, which can be measured by accessibility metrics.

2.4.1. Accessibility to Urban Functions That Meet Human Needs

The importance and priority of needs depend on each individual person, his or her social situation, and cultural background [51]. Moreover, they can change with place and time. Although a person has a wide variety of needs in everyday life, in times of catastrophic disasters, such as severe earthquakes, these are narrowed down to the most basic needs for survival and protection [47]. Therefore, in this study, the residents' accessibility to urban functions that satisfy human needs for survival and protection was set as the main criterion for measuring urban performance.

For the purpose of the city's performance evaluation, the urban system was modeled as a complex network by applying graph theory principles [74]. Graph nodes represented the centroids of building footprints, and edges between nodes were road medians connecting residential and important buildings. All edges were assumed to be bidirectional because in an emergency situation, they can provide passages in both directions. Buildings' nodes were weighted according to the number of inhabitants, and road edges were weighted according to their permeability. The graph model of the urban system allowed for the calculation of accessibility from residential buildings to important buildings via graph theory measures. Firstly, based on the data on building use and the program, residential buildings and non-residential buildings accommodating healthcare and emergency rescue services that can meet the basic needs for survival and protection were detected. Secondly, the analysis of travel times (related to the assumed average travel speed quoted in Table 2) for the shortest paths between every residential building and important buildings for the provision of healthcare and rescue services was performed using the GIS tools. After that, the accessibility to urban functions that meet human needs for survival and protection was assessed via the graph theory calculation of *global efficiency—E(G)* [50,75], which was adapted and upgraded by taking into account the inhabitants' accessibility to selected important buildings:

$$E(G)_{r-i} = \frac{1}{N_r N_i} \sum_{r \neq i \in G} \frac{w_p}{d_{ri}}, \quad (3)$$

where:

N_r is the number of residential buildings;
N_i is the number of selected important buildings (IB);
w_p is the number of people from each residential building;
d_{ri} is the shortest path [km] from each residential building to the selected IB.

2.4.2. Urban Performance over Time

For a comprehensive assessment of an urban system's response to an earthquake, it has to be observed over a longer period of time. According to the resilience function, this study analyzed urban performance through seismic scenarios at different times: before the disaster, immediately after it, after evacuation, and after a partial recovery following the removal of road closures. The state *before the disaster* means the initial state without any unusual external influences. *Immediately after* denotes the state following an earthquake when all inhabitants are at their homes, which were either affected or not, and roads are interrupted due to the impact (debris) of damaged buildings. *After evacuation* represents the state of affairs a day or a few days after the disaster, when affected inhabitants whose homes suffered D3-level damage have been evacuated to a safe space outside the observed system, while buildings are still damaged and roads blockages have not been removed yet. Thus, when assessing urban performance, only accessibility for inhabitants from buildings that suffered D1- and D2-level damage was considered. The state *after partial recovery* means that road closures have been removed (approximately one week after the disaster) while people are still being evacuated and buildings are still damaged, but the road system has been reconnected and its functionality restored. Since it is difficult to predict the exact course of the complex recovery process, the urban performance is not regarded as time-dependent, but rather refers to the events in the recovery phase (emergency evacuation and the removal of road closures). Finally, the city's performance was assessed before and immediately after the earthquake event as well as during the recovery process while taking two different scenarios into consideration.

3. Results

The application of the proposed framework enables researchers to obtain a wide variety of results, which can be used to comprehensively evaluate the resilience of an urban system and its performance in the event of an earthquake. The results of the presented case study show that even a moderate earthquake causes extensive damage and disruptions in urban system performance, while an extreme outcome of a severe earthquake with the design value of PGA 0.30 g (conservative approach) can lead to fatal consequences and irreversible damage and losses in specific areas of the city, such as the medieval core.

Damage to individual urban components is summarized in Figure 7. In the scenario of a moderate earthquake (PGA of 0.15 g), most of the buildings stay intact (51–69%). However, 6–15% of people become homeless as their homes suffer severe to complete damage (the D3 damage state), and more than a third of inhabitants (36–49%) suffer at least minor damage to their property (IN_D2 + D3). Certain road segments (3–6%) are totally blocked due to ruins, although at least 81% of the road network is fully operational. However, when taking a conservative approach to the worst-case scenario (PGA of 0.30 g), only 13% of buildings stay undamaged, while up to 85% of inhabitants suffer some damage to their buildings (IN_D2 + D3), and 3900 (57%) inhabitants lose their home. In addition, more than a quarter of the transportation network becomes impassable.

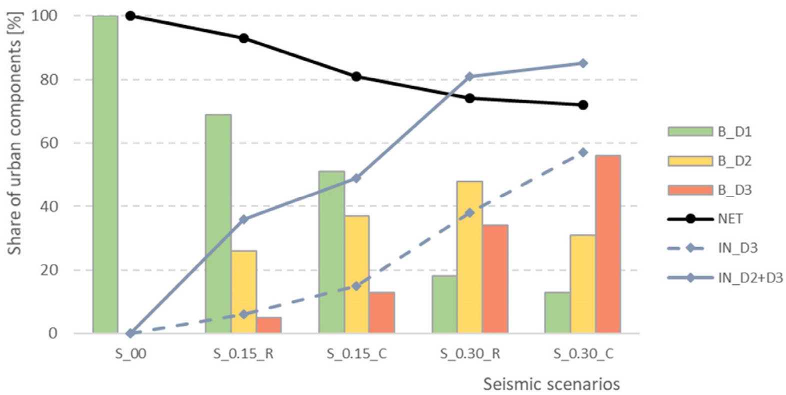

Figure 7. Obtained damage states of buildings (B_Di), road network completeness (NET), and affected inhabitants (in buildings that suffered D3 and D2 + D3 level damage) under different seismic scenarios (S_) and approaches (risky and conservative).

According to the two different approaches, conservative (C) and risky (R), greater differences were observed in the moderate scenario (0.15 g), which caused a wider range of possible consequences. Among all considered components, the road network suffered only minor changes, while buildings and their inhabitants suffered more significant losses.

Even greater losses were observed in the urban performance (Equation (3)) measured on the basis of accessibility to urban functions that meet the needs for survival and protection (Figure 8). In the severe earthquake scenario (0.30 g), the performance dropped to between 37% (risky approach) and 41% (conservative approach) immediately after the seismic event. Following the evacuation, the performance of the damaged system dropped by an additional 15%, meaning that the lowest value reached only 45% of the initial urban performance. After the removal of road closures, the performance increased to only 59–70% compared to the initial value. On the other hand, in the case of a moderate earthquake (0.15 g), the urban performance after the road network reconnection was near the baseline value (96–98%). However, considering the scenario of 0.15 g, higher deviations were observed in the states *immediately after* and *after evacuation*, when the conservative approach depicts urban performance at 77% and risky approach at as much as 90% of the baseline level.

The presented framework also allows the acquisition of various applicable results that can be used to plan actions aimed at seismic resilience enhancement. One of them, Figure 9, was created in the GIS environment and depicts road permeability and accessibility of buildings' inhabitants to important buildings (IBs) for the provision of healthcare (a health center) and rescue services (two fire stations). It shows the cumulative shortest distance (represented in terms of travel times) from each residential building to selected important facilities (IBs) ensuring that survival and protection needs are met. From the figure, it is possible to determine the most deprived and the most advantageous locations within the urban system when taking into account the possibility of fulfilling the basic needs for survival and protection. A comparison of the situation before the earthquake and after it reveals significant differences, which should be addressed when planning for the enhancement of seismic resilience.

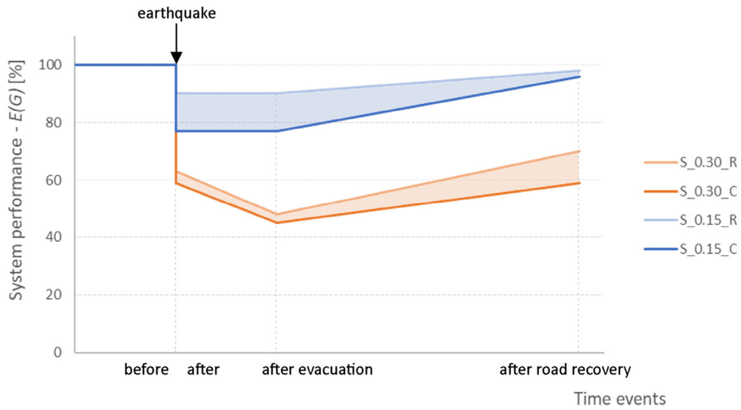

Figure 8. Simplified urban performance curve of the analysed town considered as inhabitants' accessibility to IBs (Equation (3)) over a longer period of time.

Figure 9. Cummulative accessibility to three important buildings (IBs) providing healthcare and rescue services represented as the travel time from each residential building (**a**) before (S_00) and (**b**) after a severe earthquake (S_0.30_C).

4. Discussion

The novelty of the paper is the proposal of a comprehensive interdisciplinary framework for assessing seismic urban performance, which was established by compiling narrowly focused studies and their findings. The presented framework combines seismic engineering and mathematical graph theory with sociological principles and urban planning. It places a human being at the center of interest by evaluating urban performance as a spatial capacity for satisfying basic human needs. In addition, the study offers some important improvements and supplementations of existing principles and measurements in the field of graph theory, urban performance, and seismic resilience.

In addition to the novelties, it is essential to highlight certain constraints of the research. The main focus of this paper is on the framework presentation and its verification, which is supported by a case study. As the case study is of an illustrative nature, the details and accuracy of data are not the focal point. For large building inventories on an urban scale, it is difficult to obtain consistent and detailed information. Therefore, many simplifications and coarse assumptions are often applied in existing studies. In the presented procedure, for instance, the classification of buildings is an important step. It further simplifies the assessment process and should be as precise and accurate as possible because all of the following steps depend on it. Depending only on available public data, buildings were classified regarding the structural material, height, and age, while no data on the lateral-load-resisting systems of the buildings can be found within public databases. To obtain a more accurate and segmented exposure model [76], field research would be necessary, which was beyond the scope of this research. In our case study, most of the buildings (74%) belong to only two masonry classes. Furthermore, deficient data and the reliance on the Fragility Function Manager database of fragility curves limited the ability to include specific curves for other building materials except masonry and concrete. However, steel and timber structures are rare and the majority of buildings belonging to other classes have a combination of masonry and reinforced concrete structures, which was recognized as characteristic of the Slovenian territory [8]. This rough classification could be improved by providing more detailed information and an exact calculation of structural seismic response. Furthermore, an extra class of important facilities for the provision of healthcare and rescue services, which can meet the needs for survival and protection, was defined. Although these buildings could be assigned to other classes (considering the structural material), in this study they were assumed to remain undamaged and operational, which is crucial with regards to their important function. Important facilities crucial for the functionality of the urban system require special attention and would deserve a detailed seismic analysis of their structural response in future research, whereas for the rest of the buildings, the classification into typical classes is entirely sufficient.

The accuracy of the structural seismic response prediction depends on exact classification and accurate assignment of fragility curves to different building classes. Although there is a wide range of different curves in the existing scientific literature, this study was limited to the FFM library of fragility curves [30]. This library contains 415 curves mainly for masonry and reinforced concrete structures and a few for mixed (masonry–concrete) structures. However, other materials of construction are not included. In our study, such structures were assigned to O00 and O82 building classes with the assumed vulnerability of other structures, but in further research, this could be assessed by applying fragility curves if obtained from relevant literature. It is also worth mentioning that even the selected fragility curves cannot be completely precise as many unknown parameters appear in the derivation of curves. Another simplification in the presented study was the applied harmonization process, which unifies different curves on only two limit curves and in three damage states. In addition, the harmonization process excludes the out-of-plane limit states, meaning that the effects of buildings' nonstructural damage were neglected. For the building classes of the same structural material, the fragility curves from the same author were used. To avoid the simplification of harmonization and to retain a wider range of limit states, all fragility curves (regardless of the material) from the same author should be used. However, the most accurate assessment of a building's damage due to an earthquake of a certain intensity would include a precise seismic analysis of each building's structure. This is a demanding and time-consuming procedure, which is not practically applicable as part of a large-scale urban system assessment.

In addition, it is also necessary to address the uncertainties regarding the seismic event. Simulation of an earthquake scenario is a complex analysis, which typically requires expertise in geophysics, seismology, numerical modeling, and probabilistic analyses. However, due to the interdisciplinary scope, the seismic analysis represents only a fraction of our comprehensive study and is accordingly treated with the adequate level of detail. For a more detailed study of a specific case, it would be necessary to perform simulation that considers data on seismic parameters, such as the earthquake magnitude, location, depth, focal mechanism, and soil amplification. Nevertheless, the limitations listed above are common and hardly avoidable in the studies on a large-scale urban level. The challenge for future applications of the proposed framework lies in addressing these issues to ensure the attainment of even more precise results.

The multifaceted results presented in the paper demonstrate the potential for employing the framework. When assessing the damage to the built environment, the damage state distribution of a building class was considered in order to obtain the results on the number of damaged buildings, blocked road segments, and affected inhabitants (Figure 7). These results are influenced by the variation in the building classes since each class has its own individual damage distribution and the seismic risk is specific to each building class (Table 1). On the contrary, when analyzing accessibility within the system (Figure 8), the damage distribution was not applied as it can be predicted only on the basis of a building portfolio and cannot be determined for an individual building. Therefore, the mean damage grade for a building class was taken into account, and the same damage state was applied for all buildings within the class. Moreover, to address the issue of probability in seismic assessment, the study covered a range of possible consequences by applying a conservative and a risky scenario with respect to structural design (the percentage of voids). The performance of the city is thus depicted by areas of possible range instead of just a line graph (Figure 8), which allows for a more comprehensive understanding of the potential outcomes and emphasizes the importance of considering uncertainties in seismic risk assessment.

The measure of global efficiency was recognized as suitable for urban scale assessment of overall accessibility in the urban system. It consists of a simple shortest path measure; thus, it takes into account all possible shortest paths to every selected important facility. In addition, an important contribution of the study is a proposed supplementation of the global efficiency measure, which considers the number of inhabitants in the form of weight (w_p) as well. While the original criterion of global efficiency is defined relatively and does not depend on the scale of the system, the added weight allowed us to ensure that the criterion is sensitive to the changes in the number of inhabitants as well (as a result of evacuation, migration, etc.). However, for this presentation, the observed accessibility was limited only to the important buildings for the provision of healthcare and rescue services. In further research, this can be extended to all other important urban functions that satisfy different human needs. In addition to the global efficiency, which uses a holistic approach to urban performance and captures the general state of the system, the results of local accessibility via the shortest path measure are also important (Figure 9). Local accessibility can identify critical points and bottlenecks in the system, which should be addressed in order to improve seismic resilience through bottom-up practical action.

In our case study, a big difference was observed between moderate (PGA 0.15 g) and severe (PGA 0.30 g) applied seismic scenarios. In both scenarios, significant damage to and consequences for the entire system were observed. It is of particular concern that a design ground acceleration of PGA 0.30 g caused extensive devastation of the town (38–57% of people became homeless, 34–56% of buildings were completely devastated, and 26–28% of road segments were closed), which would be difficult to restore to the initial operational level. Due to infrastructure interdependencies, the consequences for system performance were even more severe (accessibility to IB was reduced by 52–55%) compared to those presented exclusively on isolated urban components. Urban performance encompasses all of these influences between different components, including the building damage, the influence on the road system and inhabitants, and the reduced overall quality of life. Interdependencies within the system may be responsible for cascading failures and the collapse of an entire urban system. Considering the local accessibility to healthcare and rescue services, large differences within the system were detected. Prior to the disaster, the less accessible sites were on the outskirts of town, but after the earthquake event, the old city center was the most deprived part of the system with many handicapped connections. Therefore, to enhance urban resilience to earthquakes, active measures by city authorities must be aimed at these urban areas.

Within the presented framework, the system's immediate response is quite comprehensively addressed, but the challenge of how to evaluate the system's recovery phase remains. There are a few attempts to examine the post-earthquake recovery of buildings or systems in the existing literature [77–79]. However, the recovery depends on intangible urban properties, especially social structure, government and city authorities, finance, and the city configuration concerning urban open spaces. More attention should be paid to the sociological structure of the system (age, education, family status, income, assets, etc.) and especially to social capital, which is important for the overall response and recovery process. Significant progress would be achieved by including open spaces and their importance for the resilience (especially during the response and recovery phase) in the assessment process. All of these social and environmental influences on urban performance should be considered in future research. In this study, the timeline was determined according to the sequence of events (prior to the earthquake, after the earthquake, after the evacuation, etc.) (Figure 8). The recovery process was merely indicated by defining two events: evacuation of the affected inhabitants from collapsed and severely damaged buildings, and removal of road closures. The restoration of damaged buildings was not considered and remains to be addressed in future research.

Nevertheless, despite certain shortcomings, the presented framework was found to be a promising tool for a comprehensive evaluation of an urban system's resilience to earthquakes. The presented resilience assessment tends to combine quantitative and qualitative approaches while also considering intangible values that are fundamental to human prosperity and the overall quality of life. Moreover, the framework has an open structure and allows for upgrades and modifications, and it may even be adapted to a specific case study. Therefore, after taking into consideration the aforementioned limitations, it can be improved in future work to achieve a higher level of accuracy, reliability, and usability.

5. Conclusions

The paper introduces a comprehensive framework for urban performance assessment in the event of an earthquake on a city scale. The significance of the work lies in the fact that various findings from narrowly focused engineering and social studies have been assembled into a holistic framework for evaluating urban seismic performance from a human perspective. Moreover, interdependencies and interactions between different urban components (buildings—the road network—inhabitants) have been considered and evaluated based on different metric combinations ranging from seismic engineering methods (seismic demand parameters) to graph theory measures and sociological principles. Urban performance is evaluated as accessibility to basic human needs via global (the global efficiency) and local (the shortest path) indicators of graph theory. Another contribution of the study is an upgraded global efficiency measure, which reflects changes in urban performance in both relative (accessibility between pairs of buildings) and absolute (the scope of the system—the number of buildings and their inhabitants) senses. In addition, within the context of the notion of resilience, the urban performance was considered from the temporal aspect (before the event, immediately after it, after the evacuation, and after the recovery phase).

The framework has an open structure that includes building classification, vulnerability assessment (applying fragility curves), seismic scenario, damage to the built environment, interactions of damaged buildings with the road network, social and physical response of the urban system, and evaluation of a city's performance in terms of accessibility to urban services that can meet basic human needs at different stages. It was presented based on a case study of the small town of Brežice, which only served as an illustration of the proposed procedure. Therefore, a few pieces of rough data and simplifications were used in the study. For the applied earthquake scenarios, the old city center was recognized as the most vulnerable part of the analyzed city, which can be generally applied to similarly sized Mid-European towns with a medieval core. It was found that in the case of a severe earthquake (PGA of 0.30 g), the damage to individual urban components amounted to a loss of 26–57%. Moreover, due to the interdependency of various components, the seismic impact on urban performance in terms of accessibility was even more extensive (performance dropped by 55% compared to the initial value). However, when observing the recovery phase, a big difference between the two scenarios was identified. While the system in the moderate scenario almost completely recovers after the road blockages are removed, the functionality in the severe scenario is still reduced by a third compared to the initial value prior to the earthquake.

The presented paper offers a solid basis for further research. In addition to providing detailed and accurate data on physical as well as social urban components, the performance assessment should be extended to include a wider range of human needs. A greater challenge to be addressed in further research relates to how to evaluate a system's recovery phase. For this purpose, intangible urban properties, including social capital, authorities, and resources, need to be considered as well. Moreover, the inclusion of urban open spaces that reflects their importance for the overall resilience is crucially important during the response and recovery time. Finally, in addition to its scientific purpose, the presented framework may be further developed into a useful tool for decision makers who implement measures in the field.

Author Contributions: Conceptualization, methodology, validation, resources, D.K. and K.R.; formal analysis, investigation, data curation, writing—original draft preparation, visualization, K.R.; writing—review and editing, supervision, project administration, D.K. All authors have read and agreed to the published version of the manuscript.

Funding: This research was funded by the Slovenian Research Agency (Research core funding No. P5-0068).

Institutional Review Board Statement: Not applicable.

Informed Consent Statement: Not applicable.

Data Availability Statement: Not applicable.

Acknowledgments: The authors gratefully acknowledge the financial support that was received from the Slovenian Research Agency (Research core funding No. P5-0068). The authors would like to thank Martin Mikuletič for his assistance in proofreading this manuscript.

Conflicts of Interest: The authors declare no conflict of interest. The funders had no role in the design of the study; in the collection, analyses, or interpretation of data; in the writing of the manuscript; or in the decision to publish the results.

References

1. Kircher Charles, A.; Whitman Robert, V.; Holmes William, T. HAZUS Earthquake Loss Estimation Methods. *Nat. Hazards Rev.* **2006**, *7*, 45–59. [CrossRef]
2. Silva, V.; Amo-Oduro, D.; Calderon, A.; Costa, C.; Dabbeek, J.; Despotaki, V.; Martins, L.; Pagani, M.; Rao, A.; Simionato, M.; et al. Development of a global seismic risk model. *Earthq. Spectra* **2020**, *36*, 372–394. [CrossRef]
3. Pitilakis, K.; Franchin, P.; Khazai, B.; Wenzel, H. *SYNER-G: Systemic Seismic Vulnerability and Risk Assessment of Complex Urban, Utility, Lifeline Systems and Critical Facilities*; Springer: Dordrecht, The Netherlands, 2014.
4. Brandis, A.; Kraus, I.; Petrovčič, S. Nonlinear Static Seismic Analysis and Its Application to Shallow Founded Buildings with Soil-Structure Interaction. *Buildings* **2022**, *12*, 2014. [CrossRef]
5. Du, A.; Wang, X.; Xie, Y.; Dong, Y. Regional seismic risk and resilience assessment: Methodological development, applicability, and future research needs—An earthquake engineering perspective. *Reliab. Eng. Syst. Saf.* **2023**, *233*, 109104. [CrossRef]
6. Mouroux, P.; Le Brun, B. RISK-UE project: An advanced approach to earthquake risk scenarios with application to different european towns. In *Assessing and Managing Earthquake Risk: Geo-Scientific and Engineering Knowledge for Earthquake Risk Mitigation: Developments, Tools, Techniques*; Springer: Dordrecht, The Netherlands, 2006; pp. 479–508.
7. Carreño, M.L.; Cardona, O.D.; Barbat, A.H. New methodology for urban seismic risk assessment from a holistic perspective. *Bull. Earthq. Eng.* **2012**, *10*, 547–565. [CrossRef]
8. Babič, A.; Dolšek, M.; Žižmond, J. Simulating Historical Earthquakes in Existing Cities for Fostering Design of Resilient and Sustainable Communities: The Ljubljana Case. *Sustainability* **2021**, *13*, 7624. [CrossRef]
9. Silva, V.; Crowley, H.; Varum, H.; Pinho, R. Seismic risk assessment for mainland Portugal. *Bull. Earthq. Eng.* **2015**, *13*, 429–457. [CrossRef]
10. Milutinovic, Z.V.; Trendafiloski, G.S. WP4 Report Vulnerability of Current Buildings. RISK-UE Project. An Advanced Approach to Earthquake Risk Scenarios with Applications to Different European Towns. Contract: EVK4-CT-2000–00014. 2003. Available online: http://www.civil.ist.utl.pt/~mlopes/conteudos/DamageStates/Risk%20UE%20WP04_Vulnerability.pdf (accessed on 14 October 2022).
11. Zsarnóczay, A.; Deierlein, G.G. PELICUN—A Computational Framework for Estimating Damage, Loss and Community Resilience. In Proceedings of the 17th World Conference on Earthquake Engineering, 17WCEE, Sendai, Japan, 13–18 September 2020; pp. 1–12.
12. Silva, V.; Brzev, S.; Scawthorn, C.; Yepes, C.; Dabbeek, J.; Crowley, H. A Building Classification System for Multi-hazard Risk Assessment. *Int. J. Disaster Risk Sci.* **2022**, *13*, 161–177. [CrossRef]
13. Del Gaudio, C.; Ricci, P.; Verderame, G.M.; Manfredi, G. Urban-scale seismic fragility assessment of RC buildings subjected to L'Aquila earthquake. *Soil Dyn. Earthq. Eng.* **2017**, *96*, 49–63. [CrossRef]

14. Rosti, A.; Del Gaudio, C.; Di Ludovico, M.; Magenes, G.; Penna, A.; Polese, M.; Prota, A.; Ricci, P.; Rota, M.; Verderame, G.M. Empirical vulnerability curves for Italian residential buildings. *Bull. Earthq. Eng.* **2021**, *19*, 3165–3183. [CrossRef]
15. Ruggieri, S.; Calò, M.; Cardellicchio, A.; Uva, G. Analytical-mechanical based framework for seismic overall fragility analysis of existing RC buildings in town compartments. *Bull. Earthq. Eng.* **2022**, *20*, 8179–8216. [CrossRef]
16. Da Porto, F.; Donà, M.; Rosti, A.; Rota, M.; Lagomarsino, S.; Cattari, S.; Borzi, B.; Onida, M.; De Gregorio, D.; Perelli, F.L.; et al. Comparative analysis of the fragility curves for Italian residential masonry and RC buildings. *Bull. Earthq. Eng.* **2021**, *19*, 3209–3252. [CrossRef]
17. Lagomarsino, S.; Giovinazzi, S. Macroseismic and mechanical models for the vulnerability and damage assessment of current buildings. *Bull. Earthq. Eng.* **2006**, *4*, 415–443. [CrossRef]
18. Del Gaudio, C.; De Martino, G.; Di Ludovico, M.; Manfredi, G.; Prota, A.; Ricci, P.; Verderame, G.M. Empirical fragility curves for masonry buildings after the 2009 L'Aquila, Italy, earthquake. *Bull. Earthq. Eng.* **2019**, *17*, 6301–6330. [CrossRef]
19. Zucconi, M.; Romano, F.; Ferracuti, B. Typological fragility curves for RC buildings: Influence of damage index and building sample selection. *Eng. Struct.* **2022**, *266*, 114627. [CrossRef]
20. Ruggieri, S.; Tosto, C.; Rosati, G.; Uva, G.; Ferro, G.A. Seismic Vulnerability Analysis of Masonry Churches in Piemonte after 2003 Valle Scrivia Earthquake: Post-event Screening and Situation 17 Years Later. *Int. J. Archit. Herit.* **2022**, *16*, 717–745. [CrossRef]
21. Borzi, B.; Pinho, R.; Crowley, H. SP-BELA: Un metodo meccanico per la definizione della vulnerabilità basato su analisi pushover semplificate. In Proceedings of the XII Convegno L'Ingegneria Sismica in Italia ANIDIS, Pisa, Italy, 10–14 June 2007.
22. Ahmad, N.; Crowley, H.; Pinho, R. *Analytical Fragility Functions for Reinforced Concrete and Masonry Buildings and Buildings Aggregates of Euro-Mediterranean Regions—UPAV Methodology*; Department of Structural Mechanics, University of Pavia: Pavia, Italy, 2011; Volume 3.
23. Kohns, J.; Stempniewski, L.; Stark, A. Fragility Functions for Reinforced Concrete Structures Based on Multiscale Approach for Earthquake Damage Criteria. *Buildings* **2022**, *12*, 1253. [CrossRef]
24. Silva, V.; Crowley, H.; Varum, H.; Pinho, R.; Sousa, L. Investigation of the characteristics of Portuguese regular moment-frame RC buildings and development of a vulnerability model. *Bull. Earthq. Eng.* **2015**, *13*, 1455–1490. [CrossRef]
25. Formisano, A.; Florio, G.; Landolfo, R.; Mazzolani, F.M. Numerical calibration of an easy method for seismic behaviour assessment on large scale of masonry building aggregates. *Adv. Eng. Softw.* **2015**, *80*, 116–138. [CrossRef]
26. Chieffo, N.; Clementi, F.; Formisano, A.; Lenci, S. Comparative fragility methods for seismic assessment of masonry buildings located in Muccia (Italy). *J. Build. Eng.* **2019**, *25*, 100813. [CrossRef]
27. Biglari, M.; Formisano, A. Urban seismic scenario-based risk analysis using empirical fragility curves for Kerend-e-gharb after Mw 7.3, 2017 Iran earthquake. *Bull. Earthq. Eng.* **2022**, *20*, 6487–6503. [CrossRef]
28. Babič, A.; Žižmond, J.; Dolšek, M. Seismic risk of the building stock in Slovenia (Potresno tveganje stavbnega fonda v Sloveniji). *Civ. Eng. Gaz. Gradb. Vestn.* **2022**, *71*, 34–47.
29. Petrovčič, S.; Kilar, V. Seismic Vulnerability Assessment of Architectural Heritage Buildings in Slovenia (Ocena potresne ranljivosti objektov arhitekturne dediščine na območju Slovenije). *Ann. Ann. Istrian Mediterr. Stud. Ser. Hist. Sociol.* **2017**, *27*, 277–294. [CrossRef]
30. Syner-G. Available online: http://www.vce.at/SYNER-G/index.htm (accessed on 14 October 2022).
31. Zhang, W.; Chen, P.-Y.; Crempien, J.G.F.; Kurtulus, A.; Arduino, P.; Taciroglu, E. Regional-scale seismic fragility, loss, and resilience assessment using physics-based simulated ground motions: An application to Istanbul. *Earthq. Eng. Struct. Dyn.* **2023**, *52*, 1785–1804. [CrossRef]
32. Cardinali, V.; Tanganelli, M.; Bento, R. A hybrid approach for the seismic vulnerability assessment of the modern residential masonry buildings. *Int. J. Disaster Risk Reduct.* **2022**, *79*, 103193. [CrossRef]
33. Sandoli, A.; Calderoni, B.; Lignola, G.P.; Prota, A. Seismic vulnerability assessment of minor Italian urban centres: Development of urban fragility curves. *Bull. Earthq. Eng.* **2022**, *20*, 5017–5046. [CrossRef]
34. Rus, K.; Kilar, V.; Koren, D. Resilience assessment of complex urban systems to natural disasters: A new literature review. *Int. J. Disaster Risk Reduct.* **2018**, *31*, 311–330. [CrossRef]
35. Argyroudis, S.; Selva, J.; Gehl, P.; Pitilakis, K. Systemic seismic risk assessment of road networks considering interactions with the built environment. *Comput.-Aided Civ. Infrastruct. Eng.* **2015**, *30*, 524–540. [CrossRef]
36. Anelli, A.; Mori, F.; Vona, M. Fragility Curves of the Urban Road Network Based on the Debris Distributions of Interfering Buildings. *Appl. Sci.* **2020**, *10*, 1289. [CrossRef]
37. Shubandrio, F.D.; El-Maissi, A.M.; Kassem, M.M.; Masrilayanti, M.; Rahmat, S.R.; Mohamed Nazri, F. Evaluating the Interdependencies of Infrastructure Critical Systems during Earthquake Event: A Case Study for Padang City. *Sustainability* **2022**, *14*, 15926. [CrossRef]
38. Khazai, B.; Argyroudis, S.; Kakderi, K.; Taucer, F.; Hancilar, U. *Guidelines for the Consideration of Socio-Economic Impacts in Seismic Risk Analysis*; EUR 25882; Publications Office of the European Union: Luxembourg, 2013.
39. Cutter, S.L.; Ash, K.D.; Emrich, C.T. The geographies of community disaster resilience. *Glob. Environ. Chang.* **2014**, *29*, 65–77. [CrossRef]
40. Koren, D.; Rus, K. The potential of open space for enhancing urban seismic resilience: A literature review. *Sustainability* **2019**, *11*, 5942. [CrossRef]

41. D'Amico, A.; Russo, M.; Angelosanti, M.; Bernardini, G.; Vicari, D.; Quagliarini, E.; Currà, E. Built Environment Typologies Prone to Risk: A Cluster Analysis of Open Spaces in Italian Cities. *Sustainability* **2021**, *13*, 9457. [CrossRef]
42. Currà, E.; D'Amico, A.; Russo, M.; Angelosanti, M.; Cui, C.D.L.; Quagliarini, E. H-BET Historic Built Environment Typologies. Open spaces and SUOD events in the compact historic town. *VITRUVIO-Int. J. Archit. Technol. Sustain.* **2023**, *8*, 48–57. [CrossRef]
43. Abubakar, A. Towards a human-centred approach for enhancing place prosperity: Defining and operating within the basic human needs. *Open House Int.* **2022**, *47*, 190–206. [CrossRef]
44. Cardoso, R.; Sobhani, A.; Meijers, E. The cities we need: Towards an urbanism guided by human needs satisfaction. *Urban Stud.* **2021**, *59*, 2638–2659. [CrossRef]
45. Guida, C.; Carpentieri, G. Quality of life in the urban environment and primary health services for the elderly during the COVID-19 pandemic: An application to the city of Milan (Italy). *Cities* **2021**, *110*, 103038. [CrossRef]
46. Pan, S.; Zhao, Z.; Lim, H.W.; Li, N.; Fang, D. Restored quality of life-based approach (REQUALIFE) for urban seismic resilience assessment: Quantitative method. *Int. J. Disaster Risk Reduct.* **2022**, *79*, 103169. [CrossRef]
47. Rus, K.; Koren, D. Man, City, and Earthquake: An Analysis of the Accessibility to Urban Functions (Človek, mesto in potres: Analiza dostopnosti domestnih funkcij). *Archit. Bull. Arhit. Bilt.* **2022**, *232–233*, 16–21.
48. Verovšek, Š.; Zupančič, T.; Juvančič, M.; Petrovčič, S.; Svetina, M.; Janež, M.; Pušnik, Ž.; Bajec, I.L.; Moškon, M. The Aspect of Mobility and Connectivity While Assessing the Neighbourhood Sustainability. *Acad. J. Interdiscip. Stud.* **2021**, *10*, 37. [CrossRef]
49. Shang, Q.; Guo, X.; Li, J.; Wang, T. Post-earthquake health care service accessibility assessment framework and its application in a medium-sized city. *Reliab. Eng. Syst. Saf.* **2022**, *228*, 108782. [CrossRef]
50. Cavallaro, M.; Asprone, D.; Latora, V.; Manfredi, G.; Nicosia, V. Assessment of urban ecosystem resilience through hybrid social–physical complex networks. *Comput. Aided Civ. Infrastruct. Eng.* **2014**, *29*, 608–625. [CrossRef]
51. Max-Neef, M.A. *Human Scale Development: Conception, Application and Further Reflections*; The Apex Press: New York, NY, USA, 1991.
52. Ma, Y.; Wu, Z.; Liu, Z.; Zhang, M.; Aibaidula, M. Seismic Fragility Analysis of Aqueduct Structural Systems Based on G-PCM Method. *Sustainability* **2022**, *14*, 13161. [CrossRef]
53. Slovenian Environment Agency. Seismic Hazard Map. Available online: https://potresi.arso.gov.si/doc/dokumenti/potresna_nevarnost/ (accessed on 13 April 2023).
54. Wikipedia. Brežice. Available online: https://sl.wikipedia.org/wiki/Bre%C5%BEice (accessed on 16 February 2023).
55. Surveying and Mapping Authority of the Republic of Slovenia. Portal Prostor. Available online: https://www.e-prostor.gov.si (accessed on 14 October 2022).
56. Open Street Map. Available online: https://www.openstreetmap.org/#map=9/46.1504/14.9745 (accessed on 22 February 2023).
57. Google Street View. Brežice. Available online: https://goo.gl/maps/rAndP6HvfME4PwaH7 (accessed on 26 June 2023).
58. Liu, C.; Fang, D.; Zhao, L. Reflection on earthquake damage of buildings in 2015 Nepal earthquake and seismic measures for post-earthquake reconstruction. *Structures* **2021**, *30*, 647–658. [CrossRef]
59. Ma, Y.; Wang, D.; Cheng, H.; Shi, Y. Bayesian Theory-Based Seismic Failure Modes Identification of Reinforced Concrete Columns. *J. Earthq. Eng.* **2022**, *26*, 6703–6723. [CrossRef]
60. Hafner, I.; Lazarević, D.; Kišiček, T.; Stepinac, M. Post-Earthquake Assessment of a Historical Masonry Building after the Zagreb Earthquake—Case Study. *Buildings* **2022**, *12*, 323. [CrossRef]
61. Cattari, S.; Calderoni, B.; Caliò, I.; Camata, G.; de Miranda, S.; Magenes, G.; Milani, G.; Saetta, A. Nonlinear modeling of the seismic response of masonry structures: Critical review and open issues towards engineering practice. *Bull. Earthq. Eng.* **2022**, *20*, 1939–1997. [CrossRef]
62. Petrovčič, S.; Kilar, V. Seismic failure mode interaction for the equivalent frame modeling of unreinforced masonry structures. *Eng. Struct.* **2013**, *54*, 9–22. [CrossRef]
63. Azinović, B.; Koren, D.; Kilar, V. The seismic response of low-energy buildings founded on a thermal insulation layer—A parametric study. *Eng. Struct.* **2014**, *81*, 398–411. [CrossRef]
64. Fan, B.; Zhang, X.A.; Xiao, Y.; Abdulhadi, M.; Wang, X.; Shahzad, M.M. Failure Mode and Optimization for MSCSS with LRBs Based on IDA Method. *Buildings* **2022**, *12*, 998. [CrossRef]
65. Wilson, R.R.; Rojahn, C.; Sharpe, R.L. *Earthquake Damage Evaluation Data for California*; Applied Technology Council: Redwood City, CA, USA, 1985.
66. FEMA. Hazus. Available online: https://www.fema.gov/hazus (accessed on 7 January 2020).
67. Pitilakis, K.; Crowley, H.; Kaynia, A.M. *SYNER-G: Typology Definition and Fragility Functions for Physical Elements at Seismic Risk*; Springer: Dordrecht, The Netherlands, 2014.
68. Wiki. OpenStreetMap. GED4ALL. Available online: https://wiki.openstreetmap.org/wiki/GED4ALL (accessed on 26 June 2023).
69. Fajfar, P. Development of seismic codes in Slovenia (Razvoj predpisov za potresno odporno gradnji v Sloveniji). *Civ. Eng. Gaz. Gradb. Vestn.* **2017**, *66*, 83–96.
70. Zuccaro, G.; Cacace, F. Seismic vulnerability assessment based on typological characteristics. The first level procedure "SAVE". *Soil Dyn. Earthq. Eng.* **2015**, *69*, 262–269. [CrossRef]
71. Geological Survey of Slovenia. Basic Geological Map of Slovenia. Available online: https://ogk100.geo-zs.si/ (accessed on 26 June 2023).

72. Koren, D.; Rus, K. Assessment of a city's performance under different earthquake scenarios. In Proceedings of the 1st Croatian Conference on Earthquake Engineering 1CroCEE, Zagreb, Croatia, 22–24 March 2021.
73. Knez, M.; Muneer, T.; Jereb, B.; Cullinane, K. The estimation of a driving cycle for Celje and a comparison to other European cities. *Sustain. Cities Soc.* **2014**, *11*, 56–60. [CrossRef]
74. Wilson, R.J.; Watkins, J.J. *Graphs: An Introductory Approach--A First Course in Discrete Mathematics*; John Wiley & Sons Incorporated: Hoboken, NJ, USA, 1990.
75. Latora, V.; Marchiori, M. Efficient behavior of small-world networks. *Phys. Rev. Lett.* **2001**, *87*, 198701. [CrossRef] [PubMed]
76. Crowley, H.; Despotaki, V.; Rodrigues, D.; Silva, V.; Toma-Danila, D.; Riga, E.; Karatzetzou, A.; Fotopoulou, S.; Zugic, Z.; Sousa, L.; et al. Exposure model for European seismic risk assessment. *Earthq. Spectra* **2020**, *36*, 252–273. [CrossRef]
77. Cook, D.T.; Liel, A.B.; Haselton, C.B.; Koliou, M. A framework for operationalizing the assessment of post-earthquake functional recovery of buildings. *Earthq. Spectra* **2022**, *38*, 1972–2007. [CrossRef]
78. Burton, H.; Kang, H.; Miles, S.; Nejat, A.; Yi, Z. A framework and case study for integrating household decision-making into post-earthquake recovery models. *Int. J. Disaster Risk Reduct.* **2019**, *37*, 101167. [CrossRef]
79. Ghezelloo, Y.; Hokugo, A.; Tsukihashi, O. Production of gathering spaces in post-disaster recovery scenarios: Case studies from the Great East Japan Earthquake and Tsunami-2011. *City Territ. Archit.* **2023**, *10*, 11. [CrossRef]